iScience

CellPress
OPEN ACCESS

Article

Wrinkle nanostructures generate a novel form of blue structural color in great argus flight feathers

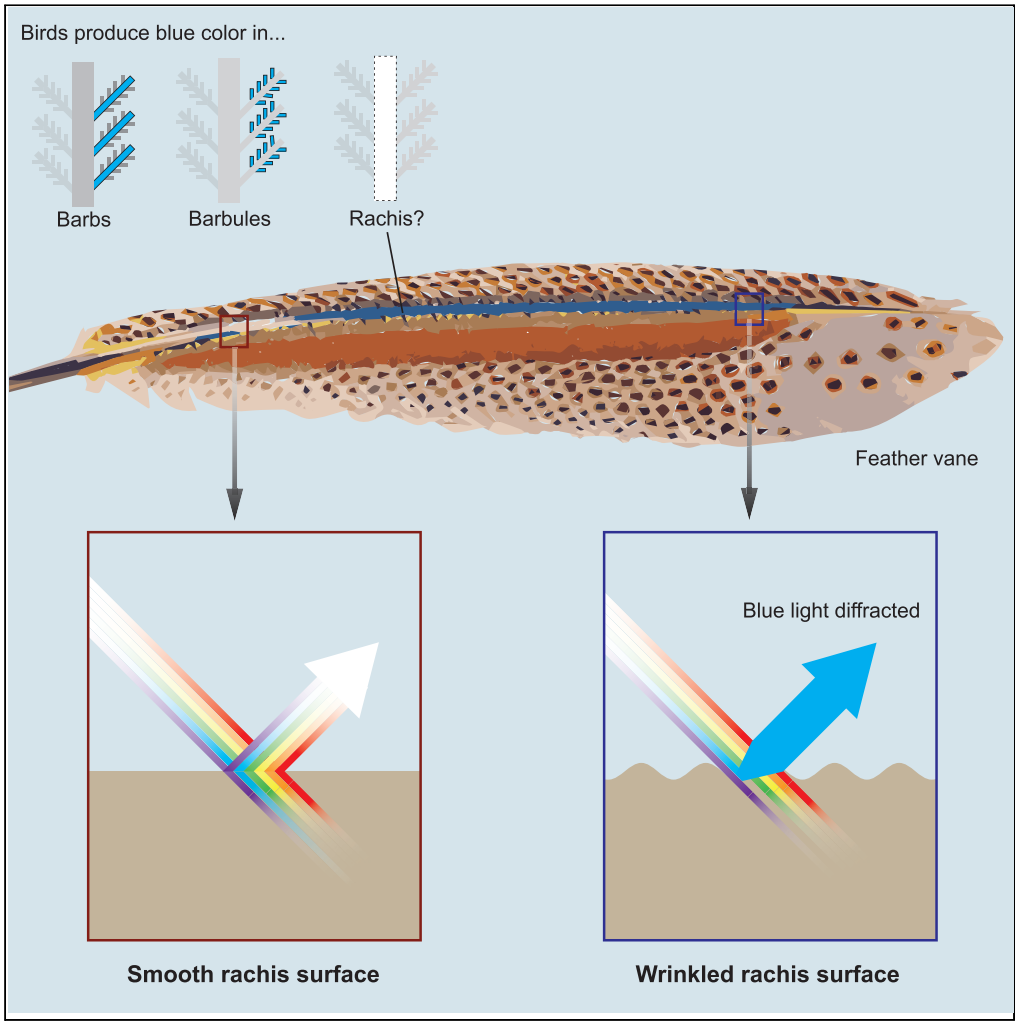

Chad M. Eliason, Julia A. Clarke, Suzanne Amador Kane

celiason@fieldmuseum.org

Highlights

The blue rachis of the great argus flight feather is covered with nanoscale wrinkles

Wrinkle nanostructures diffract blue light, a new mechanism of color production in birds

Nanostructures in crocodiles suggest shared wrinkle-producing capability in archosaurs

Eliason et al., iScience 26, 105912
January 20, 2023
https://doi.org/10.1016/j.isci.2022.105912

iScience

CellPress
OPEN ACCESS

Article

Wrinkle nanostructures generate a novel form of blue structural color in great argus flight feathers

Chad M. Eliason,[1,2,5,*] Julia A. Clarke,[3] and Suzanne Amador Kane[4]

SUMMARY

Currently known structural colors in feathers are caused by light scattering from periodic or amorphous arrangements of keratin, melanin, and air within barbs and barbules that comprise the feather vane. Structural coloration in the largest part of the feather, the central rachis, is rare. Here, we report on an investigation of the physical mechanisms underlying the only known case of structural coloration in the rachis, the blue rachis of great argus (*Argusianus argus*) flight feathers. Spectrophotometry revealed a reflectance peak at 344 nm that is diffuse and well matched to the blue and UV-sensitive cone sensitivities of this species' visual system. A combination of electron microscopy and optical modeling confirmed blue coloration is generated by scattering from amorphous wrinkle nanostructures 125 nm deep and 385 nm apart, a new avian coloration mechanism. These findings have implications for understanding how novel courtship phenotypes arise through evolutionary modification of existing ontogenetic templates.

INTRODUCTION

Some of the most diverse phenotypes are those involved in elaborate courtship displays. For example, birds such as the great argus and birds-of-paradise utilize complex visual signals, movements, and sounds to attract potential mates.[1,2] Signal traits in birds represent an ideal system for studying novelty because such traits are often complex[1] and involve interactions between genes, physicochemical traits, and functions.[3] In particular, avian feather coloration is an emergent phenotype that stems either from pigment composition or structuring of feather materials.[4] To date, all verified cases of structural coloration in feathers are generated in the smallest parts of feathers: the barbs and barbules that make up the vanes.[5,6] In feather barbs, non-iridescent structural colors are generally caused by the 3D amorphous arrangement of keratin and air into either channels or spheres.[7] By contrast, in feather barbules, iridescent structural colors are generated by thin films,[8] 1D multilayer reflectors,[9] or 2D photonic crystals.[10,11] Despite impressive variation in the size and shape of feather nanostructures, the classes of nanostructures that can form in barbs and barbules are distinct: barbules do not develop keratin-air nanostructures as seen in feather barbs, and barbs do not develop organized layers of melanosomes to coherently reflect light.[5]

The great argus (*Argusianus argus*) is a large pheasant that uses its flight feathers to form a "bowl" shape as part of a dynamic, multimodal courtship display.[12] A peculiar blue color in the central rachis of primary flight feathers first described by William Beebe in the early 20th century[12] remains the only known case of blue rachis coloration in birds. Although recently the smooth surface of the rachis of feathers of the cassowary, a large flightless bird, was shown to cause enhanced gloss (i.e., achromatic enhancement of specular vs diffuse reflection),[13] there is thus far no published evidence for nanostructures causing hue changes due to rachis-borne structural coloration. Rachis coloration in other bird species is due to pigmentation: melanin in black and brown rachises and carotenoids in the red and yellow shafts of the Northern flicker used in displays.[14] Given there are no known cases of blue pigments in feathers,[15] we hypothesized that blue rachis color is caused instead by a unique instance of structural coloration in this part of the feather. By contrast, structural colors in feather barbs and barbules have evolved independently in several groups.[5,15]

This dramatic difference in coloration mechanisms deployed in feather vanes and the rachis suggests that i) unique aspects of development, complexity, or scale of feather barbs and barbules differentially enable

[1]Negaunee Integrative Research Center, Field Museum of Natural History, Chicago, IL 60605, USA

[2]Grainger Bioinformatics Center, Field Museum of Natural History, Chicago, IL 60605, USA

[3]Jackson School of Geosciences, University of Texas at Austin, Austin, TX 78712, USA

[4]Physics & Astronomy Department, Haverford College, Haverford, PA 19041, USA

[5]Lead contact

*Correspondence: celiason@fieldmuseum.org

https://doi.org/10.1016/j.isci.2022.105912

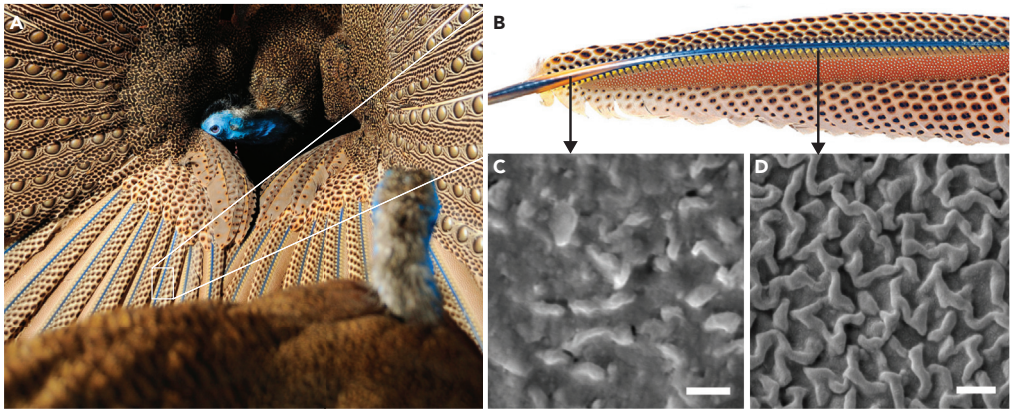

Figure 1. Wrinkle nanostructures are located in the blue part of the great argus flight feather rachis

(A) Displaying male great argus pheasant (*Argusianus argus*) showing blue coloration in primary feather rachises and approximate location of feather sampling (white box).

(B) Single flight feather showing approximate locations for SEM imaging.

(C and D) SEM images of the rachis surface revealing wrinkle structures in the blue part of the rachis (d) and absence of these structures near the base of the feather. (C) Scale bars are 500 nm (C and D). Photo credit: Jeremy Johnson CC-3.0 (A and B).

their structural diversity relative to that of the rachis, enabling a greater range of structural coloration; and/or ii) distinct ontogenic or functional constraints limit the formation of structural coloration in feather rachises. For example, hydrodynamic constraints have been implicated in barb microstructure changes in penguins (e.g., flattened barbs, loss of the central vacuole)[16] that may have excluded other mechanisms of generating blue color and led to its production via novel keratin nanofibers.[17]

A first step in studying the origin of any novel form of structural coloration is to understand the underlying physical mechanism. This approach has shed light on how nanoscale changes in feather tissue influence plumage color[10,11,17] and why some groups of birds are more colorful than others.[18,19] To study the physical mechanism of coloration in the blue rachis of the great argus, we used a combination of advanced 3D imaging, optical modeling, and Raman spectroscopy to investigate potential rachis nanostructures responsible for the blue coloration. We further compared the observed argus rachis structure with examples of similar nanostructures in another archosaur species (i.e., the clade including crocodiles and birds).

RESULTS

Scanning electron microscopy (SEM) of the blue rachis revealed a wrinkle layer only on the dorsal surface. This wrinkle layer was located atop a solid layer of keratin (Figure S1B). It consisted of ridges of keratin 178 $\pm$ 18 nm in diameter (Figure 1D). Fast Fourier transform (FFT) analysis showed a single diffraction ring, indicating these ridges are quasi-ordered; i.e., they have only short-range order along the surface (Figure 2A, inset), with a mean nearest neighbor distance of 385 nm. The observed wrinkle height was 125 nm, as measured from a 3D tomograph constructed from focused ion beam milling and SEM (Figure 2B). Wrinkle spacing estimated from FFT analysis of another archosaur integument (Nile crocodile scales) was >700 nm (see Figure 3D).

Reflectance spectrophotometry of the great argus rachis revealed a distinct diffuse peak at 344 nm that extends over a wide range of UV-blue wavelengths (Figure 2C). Peak wavelength and spectral shape were the same for all angles measured (Figure S2). Observed variation in absolute reflectance values at different angles (Figure S2) is consistent with instrument uncertainty from repositioning the reflectance probe. To determine if wrinkle nanostructures cause the observed blue color (Figure 1A), we modeled them as a sinusoidal surface (Figure 2C, inset) defined by two parameters known to determine optical performance in artificial nanostructures: wrinkle spacing and wrinkle height. Optical modeling showed that wrinkle nanostructures act as a surface diffraction grating (Figure 2C), with wrinkle height (h) modulating brightness (Figure 4A) and wrinkle spacing (λ) determining color or hue (Figure 4B). Simulated wrinkle heights greater than 200 nm or less than 50 nm caused the reflectance peak to flatten out (Figure 4A); interestingly, the argus feather was within this optimal range at h = 125 nm. While ordinary diffraction gratings can only reflect colored light at well-defined angles, our simulations show that wrinkle nanostructure reflects blue

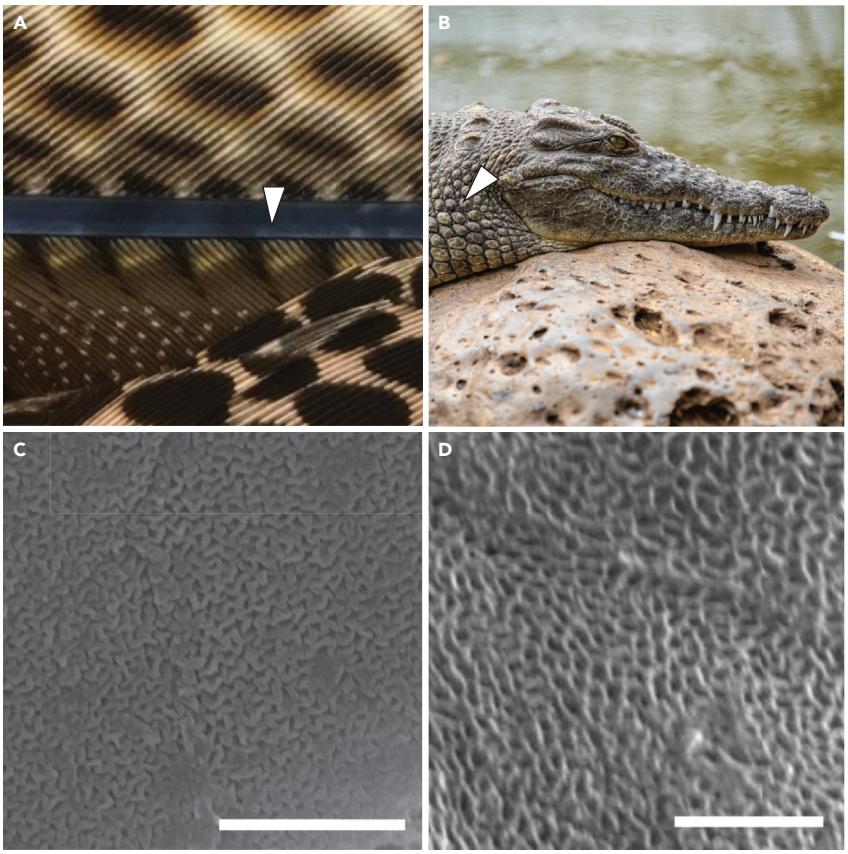

Figure 2. Comparative analysis of surficial keratin nanostructures in archosaurs

Upper images show photographs of the great argus rachis (A) and Nile crocodile scales.

(A and B) Lower images are SEM micrographs of surface nanostructures in the great argus rachis (C) and crocodile scales.

(D) All scale bars are 5 μm. Image credits: Josh Moore CC BY-NC-ND 2.0 (B) and Evan Saitta (D).

light diffusively (i.e., independent of angle) because they reflect light at a wide variety of angles (Figure S2) due to the sinusoidally varying orientation of their surfaces (Figures 2B and 2C).

To begin to understand the developmental origin of the wrinkle nanostructure layer, we used Raman spectroscopy to compare keratin chemistry between the rachis interior keratin and the outer surface where we observed blue color (Figure 5). We observed a shift in the Amide I band (Figure 5), suggestive of higher α-keratin content at the rachis surface.[20,21]

DISCUSSION

A unique mechanism and location for a color-producing nanostructure in birds

Our combined SEM, reflectance spectrum, and optical modeling results indicate that the wrinkle nanostructure found on the cortex surface of the great argus rachis indeed corresponds to a new mechanism for blue structural coloration in birds. For comparison, while achromatic structural gloss in the rachis was recently described for the rachis of the large-bodied cassowary,[13] in that case the rachis surface was smooth, not wrinkled. The reflectance peak of argus nanostructures spans a wide range of angles (Figure S2) and over a region of the UV-blue spectrum (Figure 2C) that is well matched to the UV-sensitive cones of closely related Indian peafowl (*Pavo cristatus*),[22] and therefore likely to be highly conspicuous to females during courtship displays. The wrinkle height found for these feathers also corresponds to the near-optimal value for producing a reflectance peak.

Although surface gratings generally cause color that is highly dependent on the angle of light and the viewing angle,[23] our simulation results suggest that wrinkle disorder (Figure 2A) causes reflection at

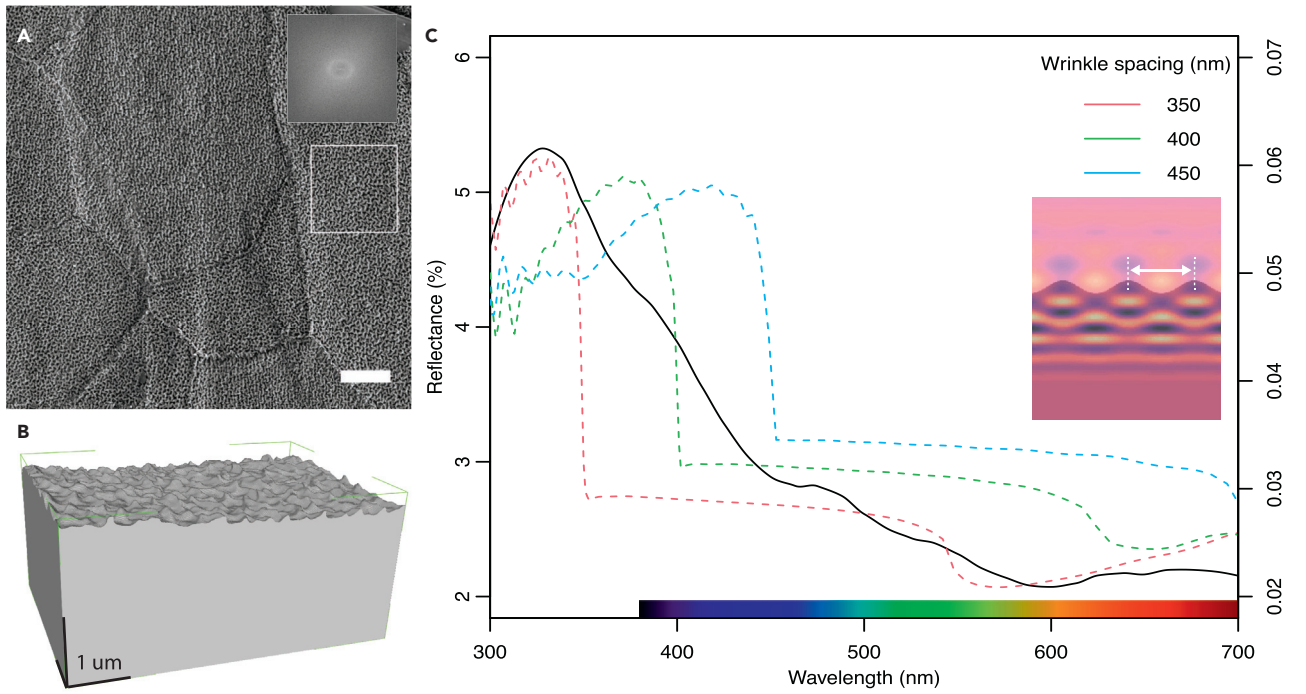

Figure 3. Diffractive mechanism of color production in great argus feathers

(A) SEM images of wrinkle nanostructures present at the rachis surface. (scale bar = 5 μm). Wrinkle nanostructures appear to be confined to cell boundaries (note irregular grooves in a) and fast Fourier transform (FFT) analysis of the structure reveals short-range order, visible as a ring in the FFT (a, inset).

(B) 3D model of wrinkle nanostructure produced using FIB-SEB. Scale bars in each dimension are 1 μm (see lower left).

(C) Reflectance spectrum of the rachis (solid black line) shows a clear 344 nm peak. Optical model results for different wrinkle spacing values are shown as colored dashed lines, assuming a sinusoidal surface grating with different spacings (see Supplemental Methods for details). Inset to (C) shows the electric field magnitude as a plane wave strikes the surface (model parameters: wrinkle height = 175 nm, wrinkle spacing = 350 nm; keratin refractive index = 1.56).

broader angles (Figure S2). Other studies have similarly reported angle-independent color that is caused by disorder in surface diffraction gratings. For example, a diffuse scattering effect has been observed in flower petals[24] and peacock spider scales,[25] in which adding small amounts of disorder to surface diffraction gratings produce blue colors visible over a range of angles. Research with artificial materials[26] has shown that disorder in wrinkle spacing (not height) causes angular broadening of diffraction peaks and rearrangement of peak intensities (i.e., certain wavelengths more pronounced than others). Given the recent interest in biomimetic design of structurally colored surfaces and materials[27–29] and the novel wrinkle structure we describe here, we anticipate the results of this study will continue to inspire the engineering design of non-iridescent color-producing structures based on wrinkling mechanisms. This is especially relevant given the growing interest in applying structural color to manufactured objects,[30] which is facilitated by methods involving only surface modifications.

Archosaurs are able to produce convergent wrinkle nanostructures

Similar wrinkle nanostructures have been described in the integument of another archosaur species: the Nile crocodile.[31] Crocodile scales had surface structures with similar degrees of quasi-ordering as the argus rachis (Figure 3D). However, wrinkle spacing for crocodile scales based on FFT analysis was >700 nm, which would, in theory, produce a peak outside the visible wavelengths of light. The evolutionary novelty in the argus rachis may be a reduction of wrinkle spacing that enables the production of bird-visible coloration, although this idea would need to be tested by rigorously comparing keratin surface structures across archosaurs. These shared features of surface keratin nanostructures among archosaurs (Figure 3) hint at a possible homology of their underlying developmental mechanisms. While wrinkle structures are widely found in living organisms,[32,33] and are actively under consideration for biomimetic applications,[24–36] this is the first example of a biophotonic (i.e., color-producing) wrinkle nanostructure in birds.

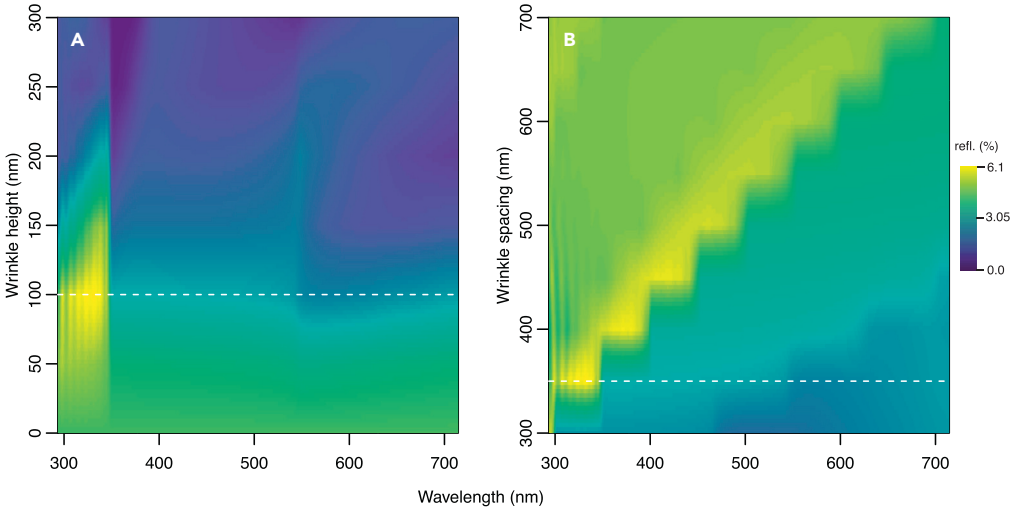

Figure 4. Simulated reflectance spectra of wrinkle nanostructures

Heatmaps showing reflectance (see legend) as a function of wrinkle height *h* (A) and wrinkle spacing λ.

(A and B) For each set of simulations, one parameter was held fixed (horizontal dashed lines) while the other parameter was allowed to vary. See STAR Methods for details and R code needed to perform optical simulations.

Hypotheses for the development of wrinkle nanostructures

Wrinkle structures form through buckling when there is a difference in elasticity and stress between adjacent layers.[37] Soft keratins (i.e., α-keratin) are known to be differentially present at scale junctures in outgroup lepidosaurs and archosaurs and in the outer feather sheath.[38] Busson et al.[39] showed evidence for four distinct layers making up the cortex of the rachis in a closely related species, the Indian peafowl. Given that our results suggest higher keratin density and a greater proportion of α-keratin at the rachis surface (Figure 5), it is possible that differences in keratin density or material properties between layers are responsible for formation of wrinkles during feather growth. Recent theoretical work on the growth of wrinkled surface layers on cylindrical structures (i.e., similar to a developing feather) suggests that differences in growth rate between layers have a small effect on wrinkle morphology compared to the difference in material properties (i.e., shear modulus) between layers.[40] An alternative developmental hypothesis is that wrinkles are formed in the keratin sheath that is preferentially retained only in the blue part of the rachis. For example, a bluish color in normally developing pin feathers and in those in which the sheath is abnormally retained[41] is superficially similar to that of the great argus rachis. The flat and wide (6 ± 0.25 mm) dorsal surface of argus rachises would be near the outer edge of the developing feather and adjacent to the feather sheath. Large rachises would result in greater surface area for rachis-sheath contact and may increase the probability of retaining portions of the feather sheath after molt. Testing these ideas will require future work on the development of wrinkle nanostructures and sheath separation in birds. Whatever the origin, once evolved, wrinkle nanostructures can produce visual signals used in elaborate courtship displays.[12]

Evolutionary implications of wrinkle nanostructures for visual signaling

If wrinkle nanostructures evolved from a shared developmental pathway in birds, why did blue rachis coloration evolve only once out of >10,000[42] recognized bird species? One possibility is that there are constraints on achieving wrinkle spacings small enough to produce bird-visible colors (i.e., less than 700 nm). Testing this idea would involve extensive SEM imaging of feather rachises across birds. A second possibility is that the rachis has evolved under strict constraints due to its key structural role. This would limit the rachis from achieving the kind of modifications allowed for barbs and barbules, which not only vary widely in coloration but also in nanostructure, number, and shape.[5] For example, mechanical constraints on the rachis's function in flight and displays have resulted in it consisting of a stiff cylindrical outer shell, the cortex, and a lightweight foam filling, the medulla.[43] However, in the unique case of the great argus, it may be that there are strong selective pressures for both structural features (large rachises) and signal properties (blue color). Our findings suggest that the great argus rachis reconciles these constraints by

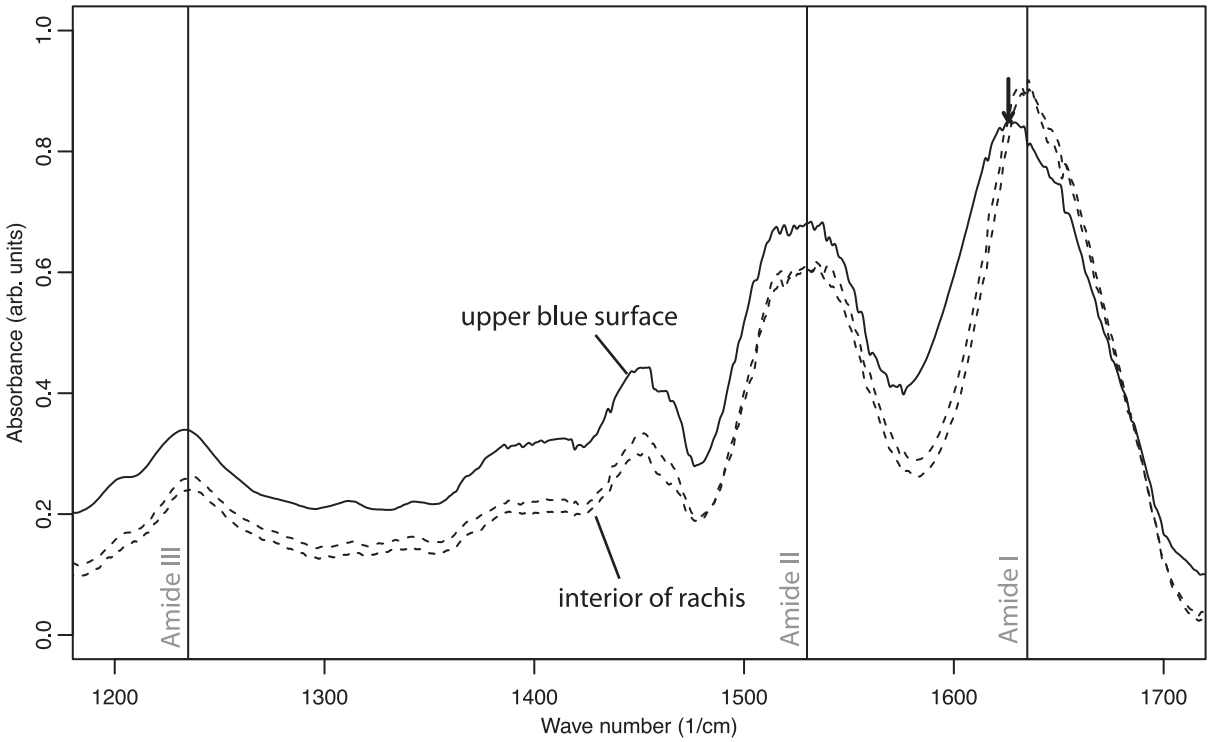

Figure 5. Raman spectroscopy of blue rachis surface

Raman spectra showing absorbance as a function of wavenumber for the interior (dashed) and exterior part of the rachis (solid line). Characteristic peaks for distinguishing different keratin forms[20] are indicated as solid vertical lines. Arrow shows location of peak shift for blue rachis in the region of the Amide I band.

generating color via a surface modification that leaves its internal structure unaffected (Figures 2B and S1B). Strong, sustained sexual selection on diverse courtship displays is another hallmark of pavonine pheasants.[12] Similar to how several pheasants utilize circular eyespots in courtship displays,[12,44] blue rachises in the great argus may accentuate feather patterns and dimensions (Figure 1A) or may involve co-option of a developmental by-product of rachis size. Behavioral work will be needed to clarify if blue rachis color is a key signal in courtship displays and whether females have innate preference for circular patterns (e.g., radiating rachises or eyespots).

Limitations of the study

We reported a novel coloration mechanism and location of structural color in the great argus pheasant (*A. argus*). To date, no other structural color has been described in the rachis of other bird species. This does not rule out the possibility that wrinkle structures are present but not capable of producing blue color. More electron microscope imaging in diverse avian species is needed to establish whether wrinkle nanostructures are more common across birds than previously recognized.

STAR★METHODS

Detailed methods are provided in the online version of this paper and include the following:

- KEY RESOURCES TABLE
- RESOURCE AVAILABILITY
  - Lead contact
  - Materials availability
  - Data and code availability
- EXPERIMENTAL MODEL AND SUBJECT DETAILS
- METHOD DETAILS
  - Feather sampling

- Reflectance spectrophotometry
- Electron microscopy
- Focused ion beam (FIB) milling
- Raman spectroscopy
- Optical modeling

- QUANTIFICATION AND STATISTICAL ANALYSIS

SUPPLEMENTAL INFORMATION

Supplemental information can be found online at https://doi.org/10.1016/j.isci.2022.105912.

ACKNOWLEDGMENTS

We thank Shannon J. Hackett, John M. Bates, Pascal Eckhoff, and Jürgen Fiebig for helpful discussions during the course of the project. Tirzah Abbott and the NUANCE center at Northwestern assisted with FIB-SEM analysis. Jack Morgan performed reflectance spectroscopy and Casey Londergan performed Raman spectroscopy analyses. This work was partially supported by the National Science Foundation (NSF EP 2112468 to C.M.E.) and Howard Hughes Medical Institute (HHMI GT10473 to J.A.C.).

AUTHOR CONTRIBUTIONS

Conceptualization, C.M.E.; Investigation, S.A.K. and C.M.E.; Formal Analysis, C.M.E.; Resources, S.A.K. and J.A.C.; Visualization, C.M.E.; Writing - Original Draft, C.M.E.; Writing - Review & Editing, C.M.E., J.A.C., and S.A.K.

DECLARATION OF INTERESTS

The authors declare no competing interests.

Received: August 17, 2022
Revised: November 15, 2022
Accepted: December 28, 2022
Published: January 20, 2023

REFERENCES

1. Ligon, R.A., Diaz, C.D., Morano, J.L., Troscianko, J., Stevens, M., Moskeland, A., Laman, T.G., and Scholes, E. (2018). Evolution of correlated complexity in the radically different courtship signals of birds-of-paradise. PLoS Biol. *16*, e2006962.

2. Davison, G.W.H. (2010). Sexual displays of the great argus pheasant Argusianus argus. Z. Tierpsychol. *58*, 185–202.

3. Eliason, C.M. (2018). How do complex animal signals evolve? PLoS Biol. *16*, e3000093.

4. Shawkey, M.D., and D'Alba, L. (2017). Interactions between colour-producing mechanisms and their effects on the integumentary colour palette. Philos. Trans. R. Soc. Lond. B Biol. Sci. *372*, 20160536.

5. Prum, R.O. (2006). Anatomy, physics, and evolution of structural colors. In Bird Coloration, *I*, K.J. Mcgraw and G.E. Hill, eds. (Harvard Univ. Press), pp. 295–353.

6. Durrer, H. (1977). Schillerfarben der vogelfeder als evolutionsproblem. Denkschr. Schweiz. nat.forsch. Ges. *91*, 1–127.

7. Prum, R.O., Torres, R.H., Williamson, S., and Dyck, J. (1998). Coherent light scattering by blue feather barbs. Nature *396*, 28–29.

8. Shawkey, M.D., Hauber, M.E., Estep, L.K., and Hill, G.E. (2006). Evolutionary transitions and mechanisms of matte and iridescent plumage coloration in grackles and allies (Icteridae). J. R. Soc. Interface *3*, 777–786.

9. Stavenga, D.G., Leertouwer, H.L., Marshall, N.J., and Osorio, D. (2011). Dramatic colour changes in a bird of paradise caused by uniquely structured breast feather barbules. Proc. Biol. Sci. *278*, 2098–2104.

10. Zi, J., Yu, X., Li, Y., Hu, X., Xu, C., Wang, X., Liu, X., and Fu, R. (2003). Coloration strategies in peacock feathers. Proc. Natl. Acad. Sci. USA *100*, 12576–12578.

11. Eliason, C.M., and Shawkey, M.D. (2012). A photonic heterostructure produces diverse iridescent colours in duck wing patches. J. R. Soc. Interface *9*, 2279–2289.

12. Beebe, C.W. (1922). Monograph of the Pheasants (H. F. & G. Witherby).

13. Eliason, C.M., and Clarke, J.A. (2020). Cassowary gloss and a novel form of structural color in birds. Sci. Adv. *6*, eaba0187.

14. Wiebe, K.L., and Moore, W.S. (2020). Northern flicker (Colaptes auratus). Birds of the World. https://doi.org/10.2173/bow.norfli.01.

15. Stoddard, M.C., and Prum, R.O. (2011). How colorful are birds? Evolution of the avian plumage color gamut. Behav. Ecol. *22*, 1042–1052.

16. Kulp, F.B., D'Alba, L., Shawkey, M.D., and Clarke, J.A. (2018). Keratin nanofiber distribution and feather microstructure in penguins. Auk *135*, 777–787.

17. D'Alba, L., Saranathan, V., Clarke, J.A., Vinther, J.A., Prum, R.O., and Shawkey, M.D. (2011). Colour-producing β-keratin nanofibres in blue penguin (Eudyptula minor) feathers. Biol. Lett. *7*, 543–546.

18. Eliason, C.M., Maia, R., and Shawkey, M.D. (2015). Modular color evolution facilitated by a complex nanostructure in birds. Evolution *69*, 357–367.

19. Eliason, C.M., Maia, R., Parra, J.L., and Shawkey, M.D. (2020). Signal evolution and morphological complexity in hummingbirds (Aves: Trochilidae). Evolution *74*, 447–458.

20. Skieresz-Szewczyk, K., Jackowiak, H., Buchwald, T., and Szybowicz, M. (2017). Localization of alpha-keratin and beta-keratin (corneous beta protein) in the epithelium on the ventral surface of the lingual apex and its lingual nail in the domestic goose (Anser Anser f. domestica) by using

immunohistochemistry and Raman microspectroscopy analysis. Anat. Rec. *300*, 1361–1368.

21. Lin, P.-Y., Huang, P.-Y., Lee, Y.-C., and Ng, C.S. (2022). Analysis and comparison of protein secondary structures in the rachis of avian flight feathers. PeerJ *10*, e12919.

22. Hart, N.S. (2002). Vision in the peafowl (Aves : Pavo cristatus). J. Exp. Biol. *205*, 3925–3935.

23. Kinoshita, S. (2008). Structural Colors in the Realm of Nature (World Scientific).

24. Moyroud, E., Wenzel, T., Middleton, R., Rudall, P.J., Banks, H., Reed, A., Mellers, G., Killoran, P., Westwood, M.M., Steiner, U., et al. (2017). Disorder in convergent floral nanostructures enhances signalling to bees. Nature *550*, 469–474.

25. Wilts, B.D., Otto, J., and Stavenga, D.G. (2020). Ultra-dense, curved, grating optics determines peacock spider coloration. Nanoscale Adv. *2*, 1122–1127.

26. Schauer, S., Schmager, R., Hünig, R., Ding, K., Paetzold, U.W., Lemmer, U., Worgull, M., Hölscher, H., and Gomard, G. (2018). Disordered diffraction gratings tailored by shape-memory based wrinkling and their application to photovoltaics. Opt. Mater. Express *8*, 184–198.

27. Shang, L., Zhang, W., Xu, K., and Zhao, Y. (2019). Bio-inspired intelligent structural color materials. Mater. Horiz. *6*, 945–958.

28. Shi, L., Zhang, Y., Dong, B., Zhan, T., Liu, X., and Zi, J. (2013). Amorphous photonic crystals with only short-range order. Adv. Mater. *25*, 5314–5320.

29. Xiao, M., Li, Y., Allen, M.C., Deheyn, D.D., Yue, X., Zhao, J., Gianneschi, N.C., Shawkey, M.D., and Dhinojwala, A. (2015). Bio-Inspired structural colors produced via self-assembly of synthetic melanin nanoparticles. ACS Nano *9*, 5454–5460.

30. Schertel, L., Magkiriadou, S., Yazhgur, P., and Demirörs, A. (2022). Manufacturing large-scale materials with structural color. Chimia *76*, 833.

31. Saitta, E.T., Rogers, C.S., Brooker, R.A., and Vinther, J. (2017). Experimental taphonomy of keratin: a structural analysis of early taphonomic changes. Palaios *32*, 647–657.

32. Tan, Y., Hu, B., Song, J., Chu, Z., and Wu, W. (2020). Bioinspired multiscale wrinkling patterns on curved substrates: an overview. Nano-Micro Lett. *12*, 101.

33. Surapaneni, V.A., Schindler, M., Ziege, R., de Faria, L.C., Wölfer, J., Bidan, C.M., Mollen, F.H., Amini, S., Hanna, S., and Dean, M.N. (2022). Groovy and gnarly: surface wrinkles as a multifunctional motif for terrestrial and marine environments. Integr. Comp. Biol. *62*, 749–761. https://doi.org/10.1093/icb/icac079.

34. Ma, L., He, L., and Ni, Y. (2020). Tunable hierarchical wrinkling: from models to applications. J. Appl. Phys. *127*, 111101.

35. Tan, A., Pellegrino, L., Ahmad, Z., and Cabral, J.T. (2022). Tunable structural color with gradient and multiaxial polydimethylsiloxane wrinkling. Adv. Opt. Mater. *10*, 2200964.

36. Zhou, L., Yang, L., Liu, Y., Xu, Z., Yin, J., Ge, D., and Jiang, X. (2020). Dynamic structural color from wrinkled thin films. Adv. Opt. Mater. *8*, 2000234.

37. Pocivavsek, L., Dellsy, R., Kern, A., Johnson, S., Lin, B., Lee, K.Y.C., and Cerda, E. (2008). Stress and fold localization in thin elastic membranes. Science *320*, 912–916.

38. Prum, R.O., and Brush, A.H. (2014). Which came first, the feather or the bird? Sci. Am. *23*, 76–85.

39. Busson, B., Engström, P., and Doucet, J. (1999). Existence of various structural zones in keratinous tissues revealed by X-ray microdiffraction. J. Synchrotron Radiat. *6*, 1021–1030.

40. Liu, R.-C., Liu, Y., and Cai, Z. (2021). Influence of the growth gradient on surface wrinkling and pattern transition in growing tubular tissues. Proc. R. Soc. A. *477*, 20210441.

41. van Zeeland, Y.R.A., and Schoemaker, N.J. (2014). Plumage disorders in psittacine birds - part 1: feather abnormalities. Eur. J. Companion Anim. Pract. *24*, 34–47.

42. Gill, F.B., and Donsker, D. (2019). IOC World Bird List (v. 9.1). http://www.worldbirdnames.org.

43. Sullivan, T.N., Wang, B., Espinosa, H.D., and Meyers, M.A. (2017). Extreme lightweight structures: avian feathers and bones. Mater. Today *20*, 377–391.

44. Kimball, R. (2001). A molecular phylogeny of the peacock-pheasants (Galliformes Polyplectron spp.) indicates loss and reduction of ornamental traits and display behaviours. Biol. J. Linn. Soc. Lond. *73*, 187–198.

45. Dalrymple, R.L., Hui, F.K.C., Flores-Moreno, H., Kemp, D.J., and Moles, A.T. (2015). Roses are red, violets are blue - so how much replication should you do? An assessment of variation in the colour of flowers and birds. Biol. J. Linn. Soc. Lond. *114*, 69–81. https://doi.org/10.1111/bij.12402.

46. Cignoni, P., Callieri, M., Corsini, M., Dellepiane, M., Ganovelli, F., Ranzuglia, G., et al. (2008). Meshlab: an open-source mesh processing tool. In Eurographics Italian chapter conference (Salerno, Italy), pp. 129–136.

47. Oskooi, A.F., Roundy, D., Ibanescu, M., Bermel, P., Joannopoulos, J.D., and Johnson, S.G. (2010). MEEP: a flexible free-software package for electromagnetic simulations by the FDTD method. Comput. Phys. Commun. *181*, 687–702.

48. Li, Y., Kovačič, M., Westphalen, J., Oswald, S., Ma, Z., Hänisch, C., Will, P.-A., Jiang, L., Junghaehnel, M., Scholz, R., et al. (2019). Tailor-made nanostructures bridging chaos and order for highly efficient white organic light-emitting diodes. Nat. Commun. *10*, 2972.

STAR★METHODS

KEY RESOURCES TABLE

REAGENT or RESOURCE	SOURCE	IDENTIFIER
SEM images	This paper	https://doi.org/10.17632/zpmrt2tmvx.1
Reflectance spectra	This paper	https://doi.org/10.17632/zpmrt2tmvx.1
Code for running optical simulations	This paper	https://doi.org/10.17632/zpmrt2tmvx.1

RESOURCE AVAILABILITY

Lead contact

Further information and requests for resources and reagents should be directed to and will be fulfilled by the lead contact, Chad M. Eliason (celiason@fieldmuseum.org).

Materials availability

This study did not generate new reagents.

Data and code availability

- Data - SEM images generated for this study have been deposited on Mendeley Data and are publicly available as of the date of publication. DOIs are listed in the key resources table. Spectral data as CSV files are also available on Mendeley Data (see key resources table).
- Code - All original code has been deposited to Mendeley Data and has been made publicly available as of the date of publication (URL available in key resources table).
- Other - Any additional information required to reanalyze the data reported in this paper is available from the lead contact upon request.

EXPERIMENTAL MODEL AND SUBJECT DETAILS

This work does not use experimental models typical in the life sciences.

METHOD DETAILS

Feather sampling

We sampled an outer (leading edge) primary feather from a male great argus (*A. argus*). Studying color mechanisms in a single feather is sufficient for characterizing structural color.[45] During display, these feathers form the elaborate bottom of a "bowl" shaped display, with secondary feathers fanning around the top such that their blue rachises form a pattern of radial blue lines (Figure 1A). We used a razor blade to cut a cross-section of the feather rachis and to remove the top layers of the rachis where the blue color originates. We also removed a brown section of the base of the rachis to use a negative control, since we did not expect nanostructures in this region.

Reflectance spectrophotometry

To measure reflectance spectra, we used a model USB2000+ spectrometer, PX-2 pulsed xenon light source and P400-1-UV-VIS optical fibers (Ocean Optics, Largo FL, USA) operating over a wavelength range of 300-700 nm, matching the visual sensitivity of closely-related Indian peafowl (*Pavo cristatus*).[22] A blue rachis specimen was illuminated at normal incidence and its reflected intensity detected at angles from 0º to 60º, in 15º increments; neither the reflectance magnitude nor wavelength distributions were found to depend significantly on reflected angle (Figure S2). All data were recorded using OceanView software (30 ms integration time, 5 scans averaged, 3 pixel boxcar averaging) in a dark, room, corrected for dark current, and normalized using a flat 99.0% reflectance standard (Spectralon USRS-99-010-EPV, Labsphere, North Sutton, NH USA).

Electron microscopy

We prepared feathers for scanning electron microscopy (SEM) by removing a small (1 mm) region of the feather surface with a razor blade. We affixed the samples to carbon tape on SEM stubs and sputter coated

the samples with gold on a Denton Vacuum Desk IV sputter coater to minimize charging. We viewed samples on a Zeiss EVO 60 SEM in the Field Museum's digital morphology laboratory.

Focused ion beam (FIB) milling

To investigate the 3-D structure of the surface nanostructures, we performed focused ion beam SEM (FIB-SEM). Briefly, we ablated 50 nm sections over a 5 μm × 5 μm area. We then reconstructed 3D surface structure using optimized threshold values in Seg3D2 (University of Utah, MIT license) and visualized the 3-D surfaces with Meshlab.[46]

Raman spectroscopy

To understand whether the chemical makeup of the surface differs from the interior, we recorded Fourier transform infrared spectroscopy (FTIR) spectra (64 scans at 2 cm^{-1} resolution) at room temperature using a Nicolet iS5 FTIR with a diamond ATR attachment. To prepare samples for FTIR, we used a paper-bladed saw to make a clean cross-section of the rachis. The paper blade avoided crushing the delicate rachis by matching its durability more closely than conventional diamond, metal, or glass blades.

Optical modeling

To test whether the observed nanoscale wrinkle structures are sufficient for explaining the observed blue color, we used finite difference time domain (FDTD) optical modeling implemented in the MEEP program.[47] We treated the surface as a sinusoidal structure using the wrinkle height (*h*) and wrinkle spacing (λ) estimated from 3D tomographic reconstruction (Figure 2B) to define the wrinkle structure.[48] We further simulated the reflectance for a range of these structural parameters bracketing these values to assess how different combinations of wrinkle height and spacing influenced the predicted reflectance spectrum (see Mendeley Data for code to run optical simulations).

QUANTIFICATION AND STATISTICAL ANALYSIS

This work does not rely on statistical analyses typical in the life sciences.